

# Break The Spell Of Total Correlation In $\beta$ -TCVAE

Zihao Chen, Qiang Li, Bing Guo, and Yan Shen

**Abstract**—This paper proposes a way to break the spell of total correlation in  $\beta$ -TCVAE based on the motivation of the total correlation decomposition. An iterative decomposition path of total correlation is proposed, and an explanation for representation learning ability of VAE from the perspective of model capacity allocation. Newly developed objective function combines latent variable dimensions into joint distribution while relieving independent distribution constraint of the marginal distribution in combination, leading to latent variables with a more manipulable prior distribution. The novel model enables VAE to adjust the parameter capacity to divide dependent and independent data features flexibly. Experimental results on various datasets show an interesting relevance between model capacity and the latent variable grouping size, called the "V"-shaped best ELBO trajectory. Additional experiments demonstrate that the proposed method obtains better disentanglement performance with reasonable parameter capacity allocation. Finally, we design experiments to show the limitations of estimating total correlation with mutual information, identifying its source of estimation deviation.

**Index Terms**—Representation learning; Unsupervised disentanglement learning; Total correlation estimation; Deep Learning

## 1 INTRODUCTION

DEEP learning has made breakthroughs in unsupervised representation learning [1],[2], speech recognition [3],[4],[5], face recognition [6],[7],[8], target monitoring [9],[10],[11],[12], and natural language processing [13],[14],[15]. These developments are largely due to the proposal on latent representation theory. Disentangled representation learning is a method of latent representation that aims to separate data features for human understanding.

Currently, many representation learning models are based on the VAE proposed by Kingma [1]. Higgins et al [16] proposed that a certain degree of penalty coefficient can be imposed on the KL term of VAE to strengthen the independence constraint of the posterior approximate distribution. R. T. Chen and Kumar A et al [2],[17],[18],[19] focused on penalizing the total correlation of the latent variables  $D_{KL}(q(z)||\prod_i q(z_i))$ , reducing the mutual information between the latent variables to achieve a good disentanglement effect. Locatello F [20] pointed out that a purely unsupervised representation learning model cannot obtain the desired disentanglement effect without giving an inductive bias. Based on Locatello's work, many representation learning models established on weakly supervised learning have appeared [21],[22],[23]. Unfortunately, it also causes the approximation error of VAE since the generation process needs to make assumptions about the distribution space of latent variables [24],[25],[26],[27].

We believe that previous works in the representation learning field have paid too much attention to the disen-

gangling capability of training a VAE, ignoring the relativity of disentangling and entangling. Disentangling results in overfitting in unsupervised learning if pursued blindly. Additionally, the VAE model's inability to directly manipulate the parameter capacity of learning independent and dependent features limits the model's parameter capacity from being effectively allocated, which lowers the model's performance.

This paper presents the  $\beta$ -STCVAE, a VAE model with the flexibility to allocate parameter capacity. We trained 100000+  $\beta$ -STCVAE models on 5 datasets (mnist, shape3D, dSprite, celebA, cars3D) and found the "V"-shaped best ELBO trajectory law between model capacity and the latent variable grouping coefficient. The experimental findings demonstrate that allocating model parameter capacity in most situations is not best addressed by implementing disentanglement constraints on the marginal distribution of latent variables. Additionally, a flaw was discovered in earlier methods for estimating the total correlation based on mutual information. We developed experiments to support our claim that the estimation error in importance sampling is caused by the difference between proposal and target distribution.

The major contributions of this paper are as follows:

- Exploring the cause of the VAE disentanglement performance by breaking down the total correlation. We discovered that there is an iterative link between local mutual information across variables and the total correlation of latent variables.
- Designing dynamic prior distribution  $\beta$ -STCVAE model that can alter the parameter capacity to learn

dependent and independent data features. This approach is motivated by total correlation decomposition. Tests on numerous datasets show that the new approach is superior in terms of learning and disentangling capabilities.

- Experiments prove that reasonable allocation of model parameter capacity can flexibly control  $\beta$ -STCVAE's disentanglement learning ability of micro and macro features. On this basis, some experimental patterns are summarized.
- Explaining the limitations of estimating total correlation based on mutual information. Confirming that the difference between proposal and target distribution in importance sampling is the source of estimation deviation.

## 2 RELATED WORKS

### 2.1 Representation Learning

The inductive preference form of the latent variable distribution  $z$  is very important in representation learning. The literature [2],[16],[17],[18],[19],[28],[29] has suggested adding regular inductive preference to the objective optimization function, thus imposing constraints on the distribution of latent variables  $z$ . Higgins et al. [20] proposed  $\beta$ VAE that imposes a strength on the ELBO's KL divergence term, encouraging the independence of each dimension in the  $z$ -space. However, the constrained potential bottleneck loses feature information when the data features pass through the encoder. The losing feature information effect reduces the representation learning ability of the model, making it difficult to achieve the best trade-off between reconstruction and feature disentangling. Some studies have proposed the decomposition of ELBO: FactorVAE [18] and  $\beta$ -TCVAE [2] proposed an encouraged posterior distribution that satisfied the factorial constraint to improve the disentangling ability of the model. Burgess [29] explained VAE from the perspective of information theory and claimed that gradually increasing the information capacity of latent variables can better balance the disentangling and reconstruction effects of the model. Joint-VAE [28] proposed a solution to the disentangling problem of discrete variables by extending the prior distribution type. DIP-VAE [17] achieved the disentangling effect by constraining the moments of the latent variable distribution.

There are also works based on a prior structured model, such as the Hierarchical depth ladder network [31],[32],[33], Data grouping disentanglement [34-39], and physical space combination [40],[41]. The disentangling based on data grouping mainly shares implicit features through artificial marking and divides the style features under the shared features. For example, ML\_VAE [34] proposed an approach that divided latent features into content and style. Weakly supervised learning artificially selects the training samples with different styles of the same content, and VAE is then used to disentangle distinct delicate styles in the same macro content. The limitation of this approach is that the VAE model cannot adjust the learning

interest when faced with real data coupled with independent and dependent features: VAE needs to use artificial labels to converge the field that model required disentangling learning.

HFVAE [33] was represented as a hierarchical model, and an iterative hierarchical model was obtained by decomposing the prior distribution terms of the ELBO. Coincidentally, the objective function proposed in this paper is similar to that of HFVAE [33]. The main difference is that HFVAE achieved the feature disentangling effect in style granularity by controlling the disentangling strength of different latent variable levels. In comparison,  $\beta$ -STCVAE directly decomposes the total correlation term and discards the disentangling constraint term of the sub-variable in HFVAE, and manipulates the allocation of parameter capacity by changing the grouping size of latent variables.

### 2.2 Vae Approximation Error

VAE approximate error analysis is primarily based on the empirical direction of the model [42],[43],[44]. The approximate error of VAE is generally caused by (1. The mismatch between the posterior and the prior distribution; (2. the problem of posterior collapse [45],[46].

Reducing the difference between the true posterior distribution and the prior is one of the main challenges. Different approaches have been proposed, such as using importance sampling to get tighter boundaries [47]; hierarchical multi-scale framework VAE; complex and scalable approximate posterior distribution [48],[49]. Most of the highlights focus on more complex target posterior distributions, leading to an increase in the complexity of the model and the computational burden of model training [27]. This paper provides a new analysis method: the parameter capacity allocation perspective. The objective function of  $\beta$ -STCVAE changes the prior distribution of latent variables by combining variables of different sizes, thus flexibly controlling the learning ability of the model to different data features.

### 2.3 Total Correlation Estimation

Statistical independence is an important indicator used in machine learning [52],[53], statistics [50],[51], and bioinformatics [54],[55] for measuring the degree of correlation between independent variables. It appears as a common regularization term in representation learning and deep learning. Mutual information is an information measure commonly used in information theory that represents the degree of randomness reduction of another independent variable when one independent variable is known. However, mutual information can only be used as an indicator to measure a pair of independent variables.

Total correlation (TC) has played an important role in representation disentanglement learning for measuring the overall correlation among multi-dimensional variables [56]. However, calculating the TC value is a major challenge because the target distribution in representation learning model is unknown and can only be estimated through sampling. Cheng P et al [57] decomposed TC and used mutual information bound to estimate the TC value.

Unfortunately, our design experiments verify that the approach in Cheng P's work[57] is inaccurate and causes estimate errors in its decomposition.

### 3 MANIPULABILITY OF PARAMETER CAPACITY AND NEW METHODS

#### 3.1 Parameter capacity allocation challenge

The real data features  $x \in \mathbb{R}^N$  are assumed to be divided into two groups: conditionally independent features  $v \in \mathbb{R}^K$  and conditionally dependent features  $w \in \mathbb{R}^H$ [16]. The conditional independent features satisfy the independent distribution  $\log p(v|x) = \sum_k \log(v_k|x)$ . It is assumed that the real data distribution can be simulated by a parametric neural network  $p(x|v, w) = \text{net}(v, w)$ , using a parametric neural network to find an inferred posterior distribution  $q(z|x)$ . The minimal complexity disentangling method between latent variables is searched during model training by constraining the total correlation, while the dependent features are loaded in a single latent variable. The disentangling of  $\beta$ -TCVAE challenges the parameter capacity allocation of neural networks. Assuming the total parameter capacity ( $Cz$ ) of the network consists of two parts: parameter capacity allocated to independent features ( $Cv$ ) and parameter capacity allocated to dependent features ( $Cw$ ), thus  $Cz = Cv + Cw$ . The parameter capacity can be effectively used only when it is properly allocated. Else the learning ability of the model will be reduced, wasting the network parameter capacity.

The following defines the typical performances that result from incorrect parameter capacity allocation in representation disentangling learning.

- Dependent feature overfitting: This is caused by  $Cw$  being too large, typically when traversing a single latent variable. The generated sample feature changes significantly and contains various features that cannot be assigned to a specific attribute or category.
- Dependent feature underfitting: This is caused by  $Cw$  being too small, typically when traversing a single latent variable. The generated samples are reconstructions of input samples with low or corrupt quality.
- Independent features overfitting: This is caused by  $Cv$  being too large. The typical performance is that two groups of generated samples are obtained when traversing two latent variables. Only slight differences in details can be regarded as entangling between the transformation methods of the two sample groups.
- Independent features Underfitting: This is caused by  $Cv$  being too small. The typical performance is that two groups of generated samples are obtained when traversing two latent variables. There are exaggerated differences between the transformation methods of the two sample groups, far beyond the subjective concept of disentangling.

Generally, when training a  $\beta$ -TCVAE model and discovering dependent feature underfitting, we will increase the learning capacity of the model (For example increase

neurons of hidden layer) while decreasing the disentangling strength  $\beta$ . Reducing the disentangling strength changes the capacity allocation method of  $Cw$  and  $Cv$ . However, determining these two hyperparameters is difficult because the value space is infinite.

Conversely, When dependent feature overfitting, we will reduce parameter capacity, and increase disentangling strength. However, large disentangling strength may lead to more latent variables becoming "passive variables"[24],[58], such variables have a standard prior Gaussian distribution with unit variance and a zero mean, which the decoder ignores during reconstruction. It is believed that such variables make the model posterior to collapse[24]. Also, reducing the parameter capacity may result in a too small  $Cw$ , causing the dependent feature underfitting.

Furthermore, although the method of parameter capacity allocation can be adjusted through disentangling strength  $\beta$ , the isotropic Gaussian prior distribution of latent variable cannot be changed, which will undoubtedly limit the effective use of parameter capacity. As discussed above, how to correctly allocate and effectively use the model parameter capacity is still a challenge.

#### 3.2 Formularization of total correlation decomposition

$\beta$ -TCVAE [2], FactorVAE [18], and DIP-VAE [17] obtain a more accurate penalty term by decomposing  $E_{p(x)}[KL(q(z|x)||p(z))]$  to achieve a trade-off of disentanglement and reconstruction.

$\beta$ -TCVAE decomposes  $E_{p(x)}[KL(q(z|x)||p(z))]$  to get the following objective:

$$D_{KL}(q(z, x_n)||q(z)p(x_n)) + D_{KL}(q(z)||\prod_i q(z_i)) + \sum_i D_{KL}(q(z_i)||p(z_i)). \quad (1)$$

It is generally believed that the disentangling ability of  $\beta$ -TCVAE [2] mainly comes from two points in objective (1): 1). The mutual information between the latent variable and the data variable represented as  $I(x; z)$  in the first item; 2). The independence between latent variables is represented as  $TC(z)$  in the second item. The third term constrains the difference between latent variable distribution and prior distribution. This paper decomposes the second item, represented as shown below: (see Appendix A.3 for the mathematical proof)

$$TC(z) = D_{KL}(q(z)||\prod_k q(z_k)) = \begin{cases} \sum_{cp(i,j)} I(z_i; z_j)|_{q(z)=q(z_i,z_j)q(z_{-i,j})} + D_{KL}(q(z)||\prod_{cp(i,j)} q(z_i, z_j)) & , n \text{ is even} \\ \sum_{cp(i,j)} I(z_i; z_j)|_{q(z)=q(z_i,z_j)q(z_{-i,j})} + D_{KL}(q(z)||\prod_{cp(i,j)} q(z_i, z_j) \cdot q(z_r)) & , n \text{ is odd} \end{cases} \quad (2)$$

Assuming that the latent variable  $z$  has  $n$  dimensions,  $z_i$  represents the  $i_{th}$  dimension in the latent variable.  $cp(i, j)$  represents a mechanism for selecting a pair of latent variables  $z_i, z_j$  without replacement.  $cp(i, j)$  in the summation symbol is consistent with the result of  $cp(i, j)$  in the cumulative multiplication symbol.  $z_r$  represents the final remaining latent variable after selecting several times without replacement under the odd case of  $cp(i, j)$ .  $p(z_{-i,j})$  represents the joint distribution probability of all

variables except the  $z_i, z_j$  latent variable.  $I(z_i; z_j)|_{q(z)=q(z_i, z_j) \cdot q(z_{-i, j})}$  represents the mutual information of  $z_i$  and  $z_j$  by important sampling when  $q(z_i, z_j)$  and  $q(z_{-i, j})$  are independent.

Explanation of each item after total correlation  $D_{KL}(q(z)||\prod_k q(z_k))$  decomposition is as follows:

The first term  $\sum_{cp(i, j)} I(z_i; z_j)|_{q(z)=q(z_i, z_j) \cdot q(z_{-i, j})}$  is the "mutual information summation" term, which represents the accumulation of mutual information combinations of all pairs  $z_i, z_j$  of latent variables selected by  $cp(i, j)$ .

The second term  $D_{KL}(q(z)||\prod_{cp(i, j)} q(z_i, z_j))$  ( $D_{KL}(q(z)||\prod_{cp(i, j)} q(z_i, z_j) \cdot q(z_r))$  is the same). This term is called the "joint distribution total correlation" term. It was discovered that the target sampling probability  $q(z)$  tends to select the samples that satisfy  $q(z_i, z_j)$  and  $q(z_{-i, j})$  are independent of each other when calculating  $I(z_i; z_j)$  in the first term. This term can be regarded as the accuracy constraint for calculating mutual information summation term, avoiding sampling bias by ensuring that the proposal sampling probability  $q(z_i, z_j)$  is not too far from the target probability during importance sampling.

Then set  $TC_{joint\_1}(z)$  as:

$$TC_{joint\_1}(z) = \begin{cases} D_{KL}(q(z)||\prod_{cp(i, j)} q(z_i, z_j)) & , n \text{ is even} \\ D_{KL}(q(z)||\prod_{cp(i, j)} q(z_i, z_j) \cdot q(z_r)) & , n \text{ is odd} \end{cases} \quad (3)$$

We replace  $\sum_{cp(i, j)} I(z_i; z_j)|_{q(z)=q(z_i, z_j) \cdot q(z_{-i, j})}$  with  $MU_{joint\_1}(z)$ , Then  $TC_{joint\_1}(z) = TC(z) - MU_{joint\_1}(z)$ .

From objective (2), knowing  $MU_{joint\_1}(z)$  is always positive, defined as the accumulation of mutual information. Thus, the total correlation of the joint distribution must be less than or equal to the total correlation of the marginal distribution, which can be represented as  $TC_{joint\_1}(z) \leq TC(z)$ .

The  $TC(z)$  decomposition has an iterative relationship and can continue by treating  $TC_{joint\_1}(z)$  as a new  $TC(z)$ . The joint distribution  $q(z_i, z_j)$  selected by  $cp(i, j)$  in the  $TC_{joint\_1}(z)$  is regarded as the new latent variable set  $\{q(z_{1,1}), q(z_{1,2}) \dots q(z_{1, n/2})\}$  ( $(n+1)/2$  variables in total when  $n$  is odd, and  $n/2$  in total when  $n$  is even), then we have:

$$\begin{aligned} TC_{joint\_2}(z) &= TC_{joint\_1}(z) - MU_{joint\_2}(z), \\ TC_{joint\_3}(z) &= TC_{joint\_2}(z) - MU_{joint\_3}(z), \\ &\dots \end{aligned} \quad (4)$$

Finally, there is the following objective:

$$TC(z) = MU_{joint\_1}(z) + MU_{joint\_2}(z) + \dots + I(z_{f,1}; z_{f,2}), \quad (5)$$

where  $f = \text{int}(\log_2 n) - 2$ . If  $f < 1$ , then  $z_{f,1} = z_i$ , and  $n$  is the total dimension of  $z$ , and  $\text{int}(c)$  is the rounded-up integer of  $c$ .

Only two joint distribution variables will be left in the final round of decomposition regardless of the parity of  $n$ . In objective (5), the remaining joint distribution of the last

term is represented by  $z_{f,1}$  and  $z_{f,2}$ .  $z_{f,1}$  and  $z_{f,2}$  are two joint distributions composed of marginal distributions selected by the  $cp(i, j)$  of the  $f$ th round. Notice that, only the mutual information  $I(z_{f,1}; z_{f,2})$  obtained in the last round of decomposition is not based on importance sampling. All  $MU_{joint\_x}(z)$  are based on importance sampling.

### 3.3 New algorithm and training method

#### 3.3.1 Training with Sampling

Due to the large sample size, each iteration to estimate  $q(z) = E_{p(x)}[q(z|x)]$  needs to traverse the entire dataset during model training. We refer to the method in R. T. Chen's work[2] for the two methods of estimating the expectation of  $\log q(z)$ :

$$E_{q(z)}[\log q(z)] \approx \frac{1}{M} \sum_{i=1}^M [\log \frac{1}{NM} \sum_{j=1}^M q(q(z|b_i)|b_j)]. \quad (6)$$

As objective (6), the first method is based on importance sampling such that when provided with a mini-batch sample set  $\{b_1, b_2, \dots, b_M\}$ .

$$E_{q(z)}[\log q(z)] = \frac{1}{N} q(z|b') + \frac{1}{M} \sum_{m=1}^{M-1} q(z|b_m) + \frac{N-M}{NM} q(z|b_M). \quad (7)$$

The second method is based on stratified sampling, which goes by the assumption that  $B_M = \{b_1, b_2, \dots, b_M\}$  are  $M$  mini-batches independently sampled without replacement. The first and second terms in objective (7) represent the estimated probability of sampling the remaining  $M-1$  samples after  $b'$  is sampled due to the independent distribution collection. The second term represents the probability of sampling  $B_M$  that does not contain  $b'$  sample.

The marginal distribution of latent variables and the local joint distribution formed between latent variables in  $\beta$ -STCVAE can be estimated using the two methods above. In the following model training, we uniformly use the method of mini-batch hierarchical sampling.

#### 3.3.2 Special case: $\beta$ -STCVAE

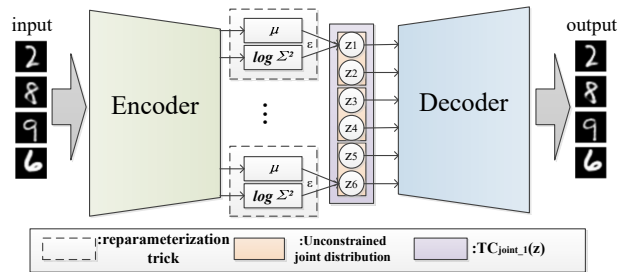


Fig. 1. The  $\beta$ -STCVAE structure is almost the same as VAE, as shown in Fig 1. The relationship of disentangling constraints between latent variables becomes more flexible. The number of the latent variable  $z$  is 6 in Fig 1. We relieve the local disentangling constraint of the adjacent pair of latent variables and get three joint distributions of latent variables (Orange area).

We can constrain  $TC_{joint\_x}(z)$  and  $MU_{joint\_x}(z)$  separately based on the decomposition process of the total correlation in 3.2.1. Intuitively, suppose the constraint of  $MU_{joint\_x}(z)$

is lifted, then  $C_w$  can be increased while  $C_z$  remains unchanged, leading to a reduction in the capacity allocated to the independent distribution features  $C_v$ .

According to the derivation in 3.2.1,  $TC(z)$  can stop decomposition at any round of iteration, and release the disentangling constraint of the first  $x-1$  term  $MU_{joint,1}(z) \sim MU_{joint,x-1}(z)$ . The total correlation disentangling penalty terms at any iteration can be written as:

$$TC_{joint,x}(z) = \begin{cases} D_{KL}(q(z) \parallel \prod_{cp(x-1,l,x-1,m)} q(z_{x-1,l}, z_{x-1,m})) & , n \text{ is even} \\ D_{KL}(q(z) \parallel \prod_{cp(x-1,l,x-1,m)} q(z_{x-1,l}, z_{x-1,m}) \cdot q(z_r)) & , n \text{ is odd} \end{cases} \quad (8)$$

where  $n$  is the number of latent variables at current iteration. If  $x-1 \leq 0$ , then  $z_{x-1,l} = z_l$ , and  $z_{x-1,m} = z_m$ .

The  $cp()$  selection function in  $TC_{joint,x}(z)$  should be specified, motivated by the decomposition of the total correlation while simplifying the calculation. The  $TC_{joint,x}(z)$  term with penalty coefficient  $\beta$  should be used to replace the total correlation term in the  $\beta$ -TCVAE loss function, and an objective with hyperparameters is designed as the loss function of  $\beta$ -STCVAE:

$$L_{\beta\text{-STCVAE}} := E_{q(z|x)p(x)}[\log p(x|z)] - I(z; x) - \beta[TC_{joint}(z)] - \sum_j D_{KL}(q(z_j) \parallel p(z_j)), \quad (9)$$

Where we take  $TC_{joint}(z)$  as  $TC_{joint,x}(z)$ 's specific goal,  $TC_{joint}(z) = D_{KL}(q(z) \parallel \prod_{j=1}^{n/i} q(z_{i(j-1)+1}, z_{i(j-1)+2}, \dots, z_{ij}))$ .  $i$  is a factor of the total dimension  $n$ , named the grouping factor.

Coincidentally, with a completely different decomposition, the loss function of  $\beta$ -STCVAE is similar to HFVAE. The HFVAE loss function can be written as:

$$L_{\text{HFVAE}} := E_{q(z|x)p(x)}[\log p(x|z)] - I(z; x) - \beta[TC_{joint}(z)] - \gamma \sum_{j=1}^{\frac{n}{i}} [TC_{joint,j}(z_{sub})] - \sum_j D_{KL}(q(z_j) \parallel p(z_j)), \quad (10)$$

Where  $TC_{joint,j}(z_{sub}) = D_{KL}(q(z_{sub}) \parallel \prod_{k=i(j-1)+1}^{ij} q(z_k))$ , and  $q(z_{sub}) := q(z_{i(j-1)+1}, z_{i(j-1)+2}, \dots, z_{ij})$ .

In the work of HFVAE, the author did not discuss how to select grouping factor  $i$  under continuous variables, but mainly studied unsupervised learning of discrete labels.  $\beta$ -STCVAE directly discards the disentangling constraints in the sub-variables grouping  $\sum_{j=1}^{n/i} [TC_{joint,j}(z_{sub})]$  compared with HFVAE, gets rid of hyperparameter  $\gamma$  that needs to be set training HFVAE.  $\beta$ -STCVAE becomes  $\beta$ -TCVAE when  $i$  equals 1. All single latent variable dimensions in  $\beta$ -STCVAE use Gaussian distribution in this paper.

From another perspective, discarding constraints  $TC_{joint,j}(z_{sub})$  makes  $\beta$ -STCVAE a dynamic prior distribution model. The prior of  $\beta$ -TCVAE is isotropic multi-dimensional Gaussian distribution, and the marginal distribution of each dimension is independent of the other. In

$\beta$ -STCVAE's prior, although the single dimension's marginal distribution is still the Gaussian distribution, independent constraints between local marginal distributions are relieved, and therefore the prior of latent  $z$  is no longer the isotropic multi-dimensional Gaussian distribution. They are  $n/i$  independent joint distributions (not necessarily multi-dimensional Gaussian distributions) composed of One-dimensional Gaussian distributions.

Intuitively, the grouping factor  $i$  should be adjusted based on the model learning scenario. The model's independent prior constraint will be smaller as  $i$  increases, and local joint distribution becomes more complex. In this case,  $\beta$ -STCVAE's encoder can learn more complex  $q(z|x)$ , which is useful for disentangling features with a high degree of complexity. For example, content classification tasks. The smaller  $i$  is, the stronger the independent constraint of the model prior is. When  $i$  equals 1,  $\beta$ -STCVAE is equivalent to  $\beta$ -TCVAE, and the prior distribution gradually becomes the multi-dimensional Gaussian distribution with independent marginal distributions. At this point, the model is more suitable for disentangling style details with lower complexity.

### 3.3.3 Classification problem and latent variable extend

When we deal with classification problems, the  $k$ -dimension latent variable can divide the data into  $k$  categories. However, when the  $\beta$ -STCVAE model is used with a grouping factor of  $n$ , the  $k/n$ -dimensional joint distribution arises, and so data can only be categorized into  $k/n$  categories. To freeze  $k$  categories, the original latent variable's dimensions should be extended to  $n^*k$  first. Then, releasing independence constraint between local marginal distributions to obtain  $k$  variables.

Extending the latent variable described above will bring a smaller total correlation of joint distributions in  $\beta$ -STCVAE. We can simply infer as following:

**Inference 1.** Assuming the amount of information in data  $x$  remains unchanged. The amount of information entropy  $H(z)$  in which the encoder network  $q(z|x)$  can obtain is also unchanged. The total correlation can be written as follows :

$$TC(z) = \sum_i H(z_i) - H(z) = D_{KL}(q(z) \parallel \prod_i q(z_i)). \quad (11)$$

The larger number  $i$  of the latent variable's dimension, the smaller amount of information that needs to be refined

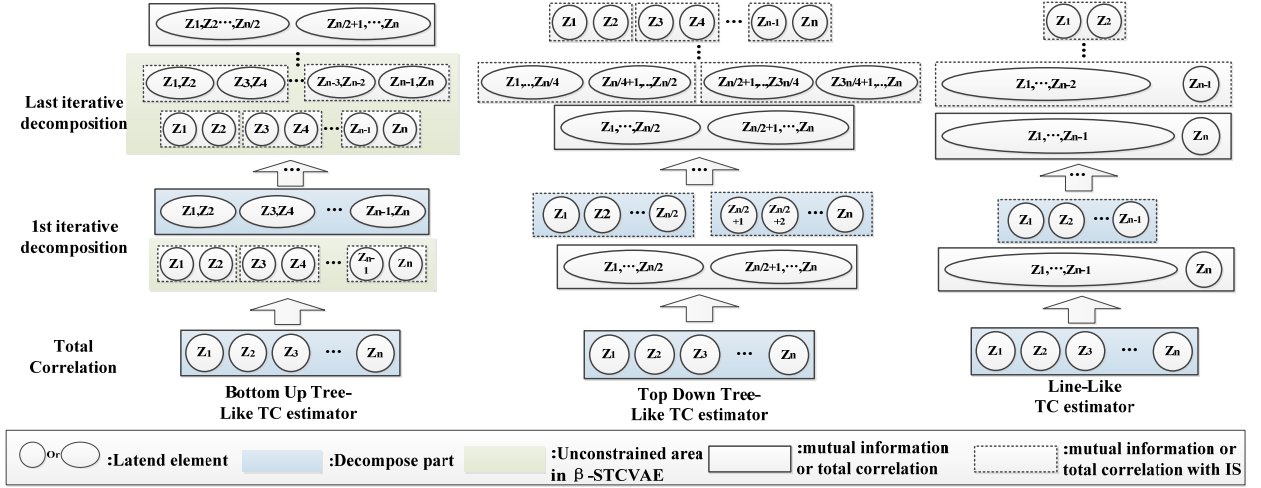


Fig. 2. Three iterative decomposition paths of TC. Suppose that latent variable  $z$  has  $n$  dimensions: the circle represents marginal distribution of a variable; the ellipse represents joint distribution of several variables; the blue color area represents the term to be decomposed from the current to the next iteration; the green color refers to the “mutual information summation” term in  $\beta$ -STCVAE where mutual information constraints are removed; the dotted line in the box refers to the total correlation item based on importance of sampling estimation.

in the average single dimension. Suppose there are two multi-dimensional latent variables  $z^i$  and  $z^j$ , their dimensions are  $i, j$ , and  $j > i$ . Then, if  $k$  satisfies  $j \geq k > i$ , the network simply needs to ensure  $H(z_k) = 0$  can lead to  $\sum_j H(z_j) = \sum_i H(z_i)$ , hence  $TC(z^i) = TC(z^j)$ .

**Inference 2.** Assuming the amount of information in data  $x$  remains unchanged. As the number of latent variables increases, so does the complexity of the encoder network  $q(z|x)$ . According to the general approximation theorem, when  $j$  is large enough, a set of  $q(z_j)$  will eventually be found to make  $D_{KL}(q(z) || \prod_j q(z_j)) = 0$ .

Therefore, when  $j = 2^*i$ , then  $TC(z^i) \geq TC(z^j)$  with a large probability, and  $TC(z^j) \geq TC_{joint\_1}(z^j)$  can be known from objective (4), so  $TC(z^i) \geq TC_{joint\_1}(z^j)$ . Validation experiment details are in Section 4.3.

### 3.4 Total correlation decomposition path

According to Cheng P[57], They proposed to use of mutual information to estimate the total correlation, which is similar to the decomposition process of the total correlation proposed in this paper. However, there are some inaccuracies in their work, and the derivation results are inconsistent with ours. Cheng P proposed the total correlation decomposition from two paths, named: Top-Down Tree-like decomposition and Line-Like decomposition.

Assuming the latent variable  $z$  has  $n$  dimensions. Then,  $n$  can be divided into two sets:  $Z_A := (z_{k1}, z_{k2}, z_{k3}, \dots, z_{km})$ ,  $Z_{\bar{A}} := (z_{v1}, z_{v2}, z_{v3}, \dots, z_{vt})$ , making  $Z = Z_A \cup Z_{\bar{A}}$ ,  $Z_A \cap Z_{\bar{A}} = \emptyset$ . The Top-Down Tree-like decomposition is written as follows in Cheng P’s work:

$$TC(Z) = TC(Z_A) + TC(Z_{\bar{A}}) + I(Z_A; Z_{\bar{A}}). \quad (12)$$

Following our derivation (see Appendix A.1 for the mathematical proof), it can be deduced that  $E_{p(Z_A)}[p(Z_{\bar{A}}|Z_A) \cdot \log(\frac{p(Z_A)}{p(z_{k1})p(z_{k2}) \dots p(z_{km})})]$  is regarded as the total correlation of  $Z_A$  in Cheng P’s work. However, we regard  $p(Z_{\bar{A}}|Z_A)$  in the above term as the important weight  $w$ .

From the fact that  $w$  is equal to 1 when  $Z_A$  and  $Z_{\bar{A}}$  are independent. It can be inferred that  $E_{p(Z_A)}[p(Z_{\bar{A}}|Z_A) \cdot \log(\frac{p(Z_A)}{p(z_{k1})p(z_{k2}) \dots p(z_{km})})]$  is the total correlation of  $Z_A$ , obtained by importance sampling when  $Z_A$  and  $Z_{\bar{A}}$  are independent. We will write it as  $TC(Z_A)|_{q(z)=q(Z_A) \cdot q(Z_{\bar{A}})}$ . Similarly, when  $Z_A$  and  $Z_{\bar{A}}$  are independent,  $E_{p(Z_{\bar{A}})}[p(Z_A|Z_{\bar{A}}) \cdot \log(\frac{p(Z_{\bar{A}})}{p(z_{v1})p(z_{v2}) \dots p(z_{vt})})]$  can be regarded as the total correlation of  $Z_{\bar{A}}$ . We will write it as  $TC(Z_{\bar{A}})|_{q(z)=q(Z_A) \cdot q(Z_{\bar{A}})}$ .

Thus, Top-Down Tree-like path decomposition should be written as follows:

$$TC(Z) = TC(Z_A)|_{q(z)=q(Z_A) \cdot q(Z_{\bar{A}})} + TC(Z_{\bar{A}})|_{q(z)=q(Z_A) \cdot q(Z_{\bar{A}})} + I(Z_A; Z_{\bar{A}}). \quad (13)$$

Similar to Top-Down Tree-like path decomposition, the correct result of the Line-Like path decomposition should be as follows (see Appendix A.2 for the mathematical proof):

$$TC(Z_{1:n}) = I(Z_{1:n-1}; Z_n) + TC(Z_{1:n-1})|_{q(z)=q(Z_n) \cdot q(Z_{1:n-1})}. \quad (14)$$

The proposed decomposition path in this paper (see Appendix A.3 for the mathematical proof) is called the Bottom-Up Tree-like path. Fig. 2 shows that the final results obtained by Top-Down and Bottom-Up Tree-like paths are the same, but intermediate decomposition paths differ. Top-Down Tree-like divides the latent variables into two groups and then computes the mutual information and total correlation between the two groups. The total correlation based on importance sampling is used as an entrance for iterative decomposition. Except for the first round of iterations, each round of iteration divides the total correlation into two, resulting in no total correlation item including all latent variable dimensions during the intermediate process. In comparison, for each round of decomposition iteration in the Bottom-Up Tree-Like path, a new joint distribution in the current round is constructed by pairing the previous round’s distribution. The disentangling constraints between overall joint distributions still exist even if  $\beta$ -STCVAE releases the disentangling constraints within

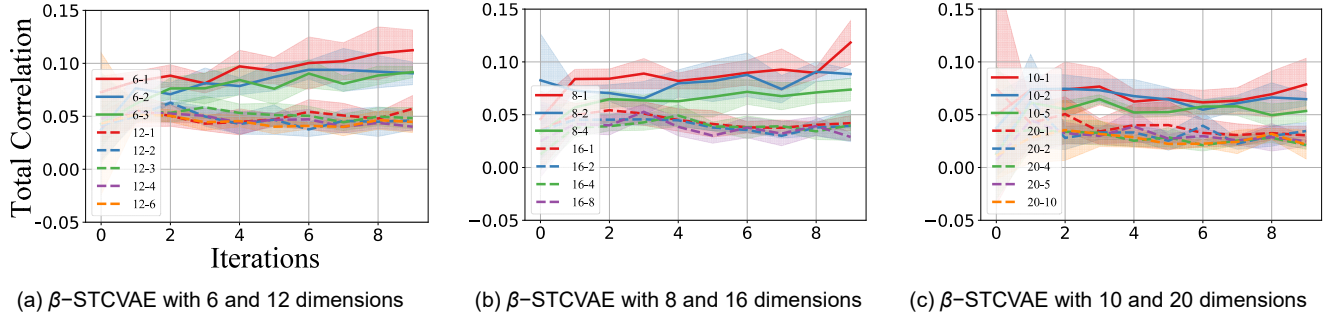


Fig. 3. Tendency of TC value from  $\beta$ -STCVAE under different grouping factor  $i$ . Model writing method: latent variable dimension\_Grouping factor, for example 16\_4 represents  $\beta$ -STCVAE model with 16 latent variable dimension, and the grouping factor is 4.

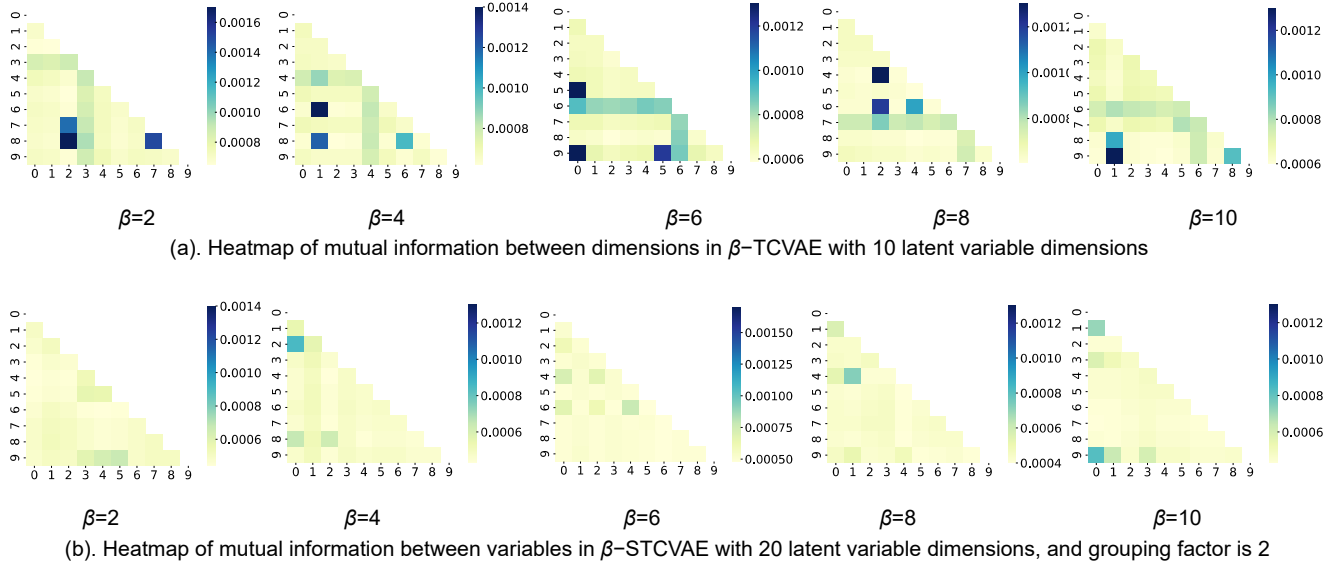


Fig. 4. Mutual information heatmap between paired variables experiment

the local joint distribution of latent variables.

In disentanglement representation learning, we need to induce stronger independence between the style and the class, while allowing correlation between the individual style dimension  $s$ . [33] Therefore, the proposed decomposition method of the Bottom-Up path is more suitable than the Top-Down path for application in representation disentangling missions. Additionally, the TC value in each round of Bottom-Up iterative decomposition is accurate and not affected by the difference between the proposal and target distribution in the importance sampling estimation.

Through the above derivation, we found that these approaches to total correlation estimation have certain scenario limitations due to the use of important sampling-based estimates in the decomposition. Based on the Bottom-Up path decomposition method,  $\beta$ -STCVAE discards the estimation based on the importance sampling part to release the local disentangling constraint, bringing an accurate total correlation luckily. However, in other usage scenarios, the estimated error may become larger if the difference between the proposal and the target distribution is

too large.

## 4 EXPERIMENT

### 4.1 Basic Settings

We analyze the feasibility and disentangling performance of  $\beta$ -STCVAE on five datasets, dSprites [16], celebA [2], shapes3d [18], cars3d [59], and mnist [60].

The experiment's neural network model parameter setting is presented in Appendix B.1 as Table1 and Table2.

### 4.2 MIG calculation on $\beta$ -STCVAE model

We use MIG to evaluate the disentangling metric. Assuming latent variable  $z$  has  $m$  dimensions, latent variable dimensions are combined into  $t$  joint distribution groups, as  $Z_A := (Z_{A1}, Z_{A2}, \dots, Z_{At})$ .  $Z_{Ai} := (z_{u_i}, z_{j_i}, \dots, z_{o_i})$  represents joint distribution  $Z_{Ai}$  composed of latent variable dimensions  $z_{u_i}, z_{j_i}, \dots, z_{o_i}$ .

If  $\forall Z_{Ai}, Z_{Aj} \in Z_A$  and  $Z_{Ai} \cap Z_{Aj} = \emptyset$ , then  $Z = Z_{A1} \cup Z_{A2} \dots \cup Z_{At}$ , and  $q(z_{Ai}, v_k) = \sum_{n=1}^N p(v_k) p(n|v_k) q(z_{Ai}|n)$ .

Statistics  $p(v_k)$  and  $p(n|v_k)$  through empirical distributions.  $X_{v_k}$  represents the set of training samples with  $v_k$  features; therefore, the mutual information of  $z_{Ai}$  and  $v_k$  as follows:

$$I(z_{Ai}; v_k) = E_{q(z_{Ai}, v_k)} \left[ \log \sum_{n \in X_{v_k}} q(z_{Ai}|n) p(n|v_k) \right] + H(z_{Ai}), \quad (15)$$

where  $H(z_{Ai})$  can be obtained using the mini-batch hierarchical sampling in Section 3.3.1. The complete MIG formula is as follows:

$$1/K \sum_{k=1}^K \frac{1}{H(v_k)} (I(z_{Ai(v_k)}; v_k) - I(z_{s_{Ai(v_k)}}; v_k)), \quad (16)$$

where  $z_{Ai(v_k)} = \operatorname{argmax}_{Ai} I(z_{Ai}; v_k)$ . Based on  $z_{Ai(v_k)}$ , there is  $z_{s_{Ai(v_k)}} = \operatorname{argmax}_{s_{Ai \neq Ai(v_k)}} I(z_{s_{Ai}}; v_k)$ .

### 4.3 Iterative decomposition of total correlation

The models compared in Fig. 3(a) have 6 and 12 latent variable dimensions; The models compared in Fig. 3(b) have 8 and 16 latent variable dimensions; The models compared in Fig. 3(c) have 10 and 20 latent variable dimensions. All disentangling strength is set at 10. Models are trained using the MLP neural network on the mnist dataset, Layer takes 1, neuron\_num takes 3000, and Latent\_dim list is [6, 8, 10, 12, 16, 20]. A single round of experiments had 10000 iterations; the training was repeated 50 times under each hyperparameter setting to draw the 90% confidence interval.

Fig. 3 shows the trend of the total correlation during model training with various grouping factors. It can be concluded from experiments that as the grouping factor in the  $\beta$ -STCVAE increases, the total correlation decreases when the latent dimension is held constant. Increasing latent\_dim will also lower the model's total correlation.

The mutual information heatmap between paired variables experiment is shown in Fig. 4. For a more intuitive comparison, with the same disentangling coefficient in both methods, the color bar's upper and lower bounds are the same. Models are trained using the MLP neural network on the mnist dataset. Mutual information between variables in Fig. 4(b) is significantly smaller than that in Fig. 4(a).

The above two experiments verify the correctness of our total correlation decomposition in 3.2, and inferences in Section 3.3.3: 1). The total correlation of joint distribution must be less than or equal to the total correlation of marginal distribution that composes the joint distribution. 2) Extending the latent variable's dimensions will lead to a smaller total correlation of joint distributions.

## 4.4 Parameter capacity allocation experiment

### 4.4.1 Optimal parameter capacity allocation

We designed the optimal capacity allocation experiment to observe the effect of latent variable grouping factor size on learning ability. The optimal ELBO with various parameter

capacities is revealed by varying the latent variable grouping factor. We performed the experiments on five different datasets. The unified experimental setting is as follows:

- The selection list of latent variable dimensions is [6, 8, 10, 12, 14, 16, 18, 20].
- 20000 iterations for a single training round.
- A single model is repeatedly trained for 20 rounds to ensure accuracy.

Model and parameter capacity list for different datasets refers to appendix B.1 Table4. We tested the model's performance under each parameter capacity composed of each factor (except  $n$  itself) of the dimension number  $n$ . For example, when the dimension is 12, grouping factors' list is [1, 2, 3, 4, 6]. The  $\beta$ -STCVAE is equivalent to  $\beta$ -TCVAE when grouping factor equals 1. It is necessary to normalize grouping factors to get a unified view of parameter capacity allocation under a different number of latent variables. Taking the largest factor  $m$  of the grouping factors as the normalization constant, all the selected grouping factors  $i$  are recorded as  $i/m$  in the experimental results, becoming a coefficient less than or equal to 1 and greater than  $1/m$ , called the latent variable  $z$ 's grouping coefficient. When the dimension is 12, the experimental grouping coefficient list is [1/6, 2/6, 3/6, 4/6, 6/6]. The grouping coefficient represents the parameter capacity allocation of the model. The larger the grouping coefficient, the stronger the learning ability of independent features. Conversely, the smaller the grouping coefficient, the stronger the learning ability of independent features. We recorded the grouping coefficient of the best ELBO under each parameter capacity and

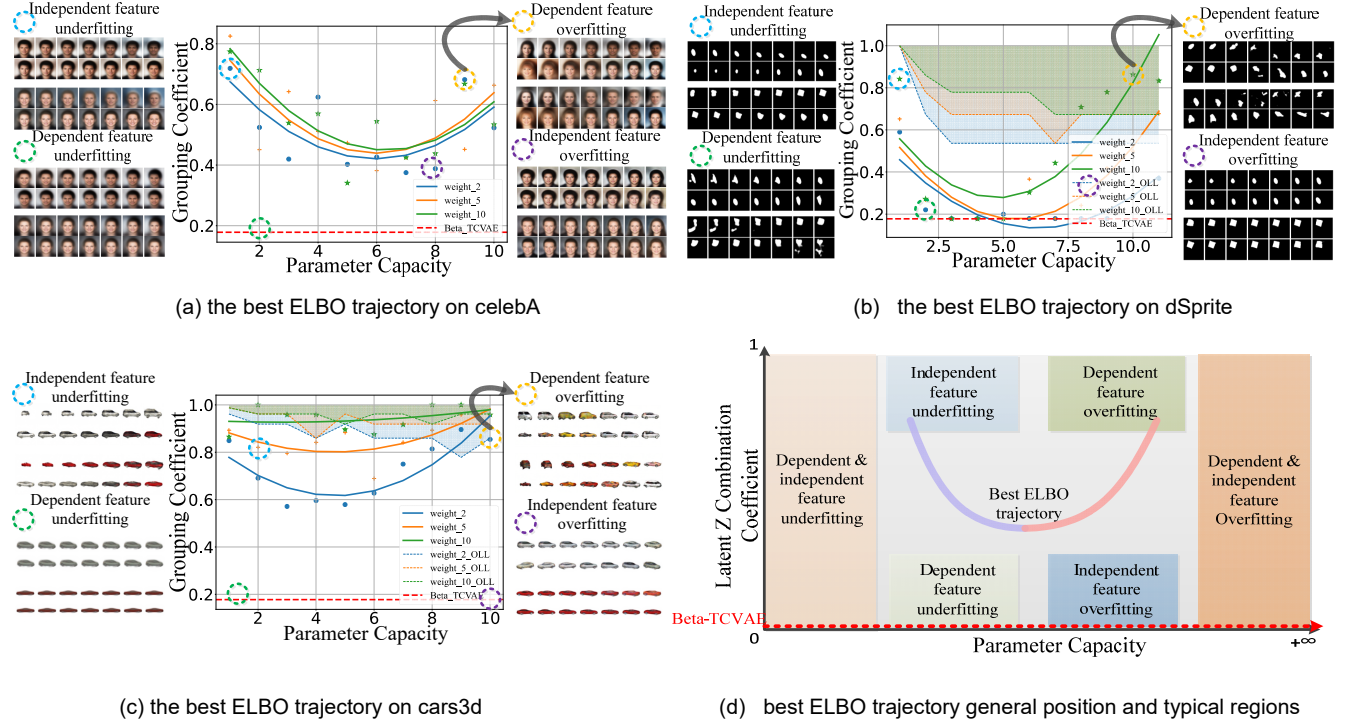


Fig. 5. The Fig. 5(a),(b),(c) plot the best ELBO trajectory of the model under different parameter capacities on datasets. The red dotted line below the figure represents  $\beta$ -TCVAE when the grouping factor is 1. Grouping coefficients corresponding to  $\beta$ -TCVAE in different dimensions are inconsistent, so we take the average value 0.178 as the drawing reference (The red dotted line below the Figs). Except for the dSprites training set,  $\beta$ -TCVAE is not on the ideal ELBO trajectory, regardless of how parameters and disentangling coefficients are altered in the datasets. The left and right of each Figs are images generated by latent traversing at 4 distinct regions (sampling in the circular dotted area). The lower Fig. 5(d) shows a general position of the optimal ELBO trajectory and indicates the approximate generation regions for six kinds of typical samples. In dSprites, cars3d, and shape3d, we marked the occurrence region (\_OLL color area in the Fig. 5(b) and Fig. 5(c)) of omniscient latent variable when  $\epsilon=0.001$  and  $\delta=0.01$  under various disentangling strengths.

plotted the average best ELBO trajectory under different parameter capacities.

We trained 100000+  $\beta$ -STCVAE models on five datasets; Use a binary function curve to fit these optimal ELBO points. Intriguingly, V-shaped pattern was found on every dataset. Fig. 5 shows that  $\beta$ -STCVAE can always obtain better ELBO than  $\beta$ -TCVAE (red dotted line) except for some situations in the dSprites dataset, regardless of disentangling strength and parameter capacities.

**Interpretation of the V-shaped optimal ELBO trajectory.**

Learning dependent data features require more than the parameter capacity assigned to a single latent variable when the total parameter capacity is low. Optimal ELBO tends to release local disentangling constraints to learn more data features. However, the parameter capacity assigned to a single latent variable dimension rises along with the gradually increasing total parameter capacity. So, the grouping coefficient of the best ELBO decreases as total parameter capacity gradually increases (purple line area of Fig. 5(d)). When a critical point is reached, because the features learned by the model parameter capacity are complex enough, a matching complex latent variable distribution is required to accommodate the features. Therefore, the one-dimensional Gaussian distributions are combined to create a more complex joint distribution, causing the grouping coefficient under the best ELBO to rise again

(pink line area of Fig. 5(d)). Additionally, we discovered that as the disentangling strength increases, the optimal ELBO trajectory moves up. This effect implies that the model allocates more parameter capacity to learn dependent features as a balancing mechanism to counteract the high disentangling strength.

**Typical generated sample characteristics in different regions.** After the generation of numerous samples from various datasets, we can summarize the following rules (Refer to Fig. 5(d)):

- Underfitting area of independent features & dependent features on the left of Fig. 5(d): the generated sample features are low-quality fuzzy reconstructions.
- Overfitting area of independent features & dependent features on the right side of Fig. 5(d): The generated sample features try to accommodate all sample features on a single latent variable, and the reconstructed output cannot identify the original input sample.
- The upper left is the independent feature underfitting regions; the lower left is the dependent feature underfitting regions; the upper right is the independent feature overfitting regions; the lower right is the independent feature overfitting regions. The generative features of these four regions are mentioned in 3.1.

Correctly assigning the grouping factor remains a difficult problem, but the regional characteristics of generated

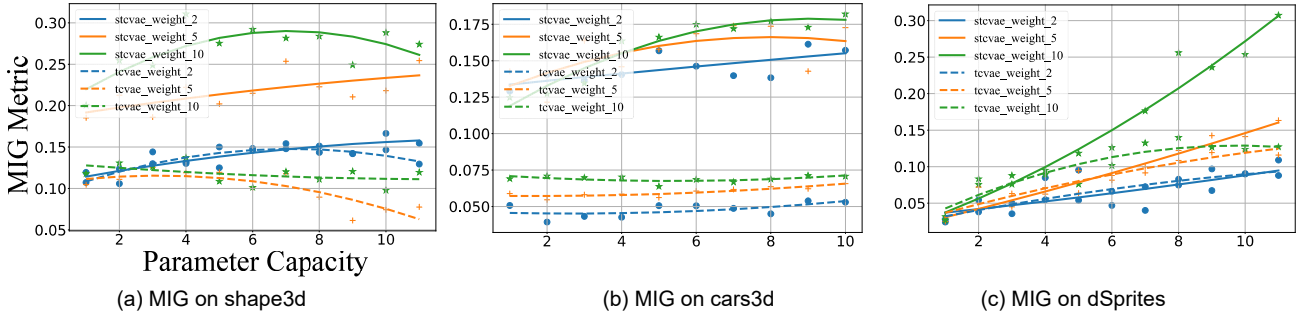


Fig. 6. The left, middle, and right are the average MIG of the two models under different parameter capacities on shape3d, cars3d, and dSprites datasets.

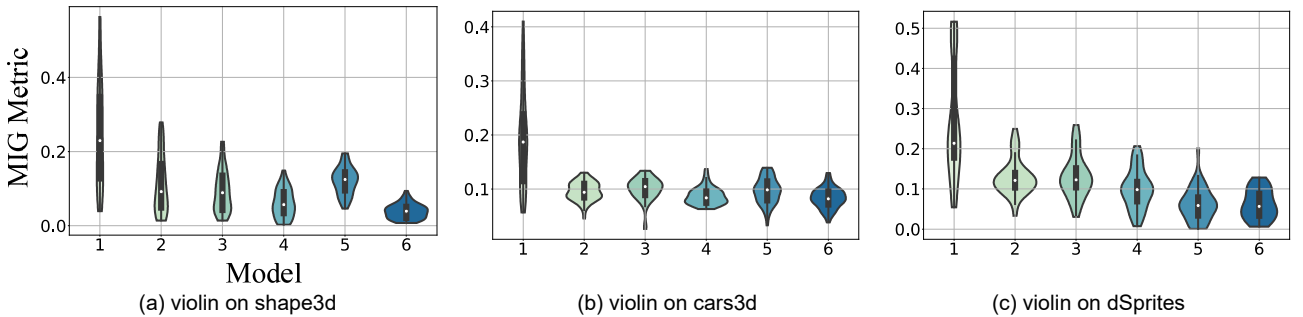


Fig. 7. The Fig. 7(a), Fig. 7(b) and Fig. 7(c) are the MIG-based disentangling metric violin graphs of different VAE models on shape3d, cars3d, and dSprites datasets. Models are abbreviated (1=StcVae\_8\_2, 2=TcVae\_16, 3=TcVae\_8, 4=BetaVae\_8, 5=FactorVae\_8, 6=DIP-I\_8). Abbreviated writing method: Model name\_latent variable dimension\_Grouping factor. For example, Stcvae\_8\_2 represents a Stcvae model with 8 latent variables when the total number of latent dimensions is 16, and the grouping factor is 2. TcVae\_8 represents a TcVae model with 8 latent dimensions.

samples can be referred to manipulate the degree of disentangling. When classifying distinct types of samples, the parameters should be near the independent feature underfitting region in the upper left corner. Conversely, when decoupling the styles within a category, make the model parameters in the lower right independent feature overfitting area. This also explains the Experimental results in [33]. We speculate: The latent traversing of HFVAE can better decouple the subtle data style than  $\beta$ VAE because HFVAE appears in the lower right independent feature overfitting region by adjusting the two-level disentangling strengths.

**Omniscient latent variable.** In the experiment, we discovered that when the latent variable grouping factor reaches a certain value threshold, the latent variable will become overloaded with data features if the parameter capacity is large enough. The phenomenon is manifested as the dependent features overfitting during latent traversing on the latent variable, called the omniscient latent variable. So, we try to locate the occurrence range of this phenomenon in cars3D, dSprites, and shape3D datasets with ground true factor labels. We found that when calculating the latent variable marginal and conditional entropy, the omniscient latent variable behaves as a variable whose information entropy is 0. Meaning the variable cannot provide any information because it attempts to contain the characteristic states of all samples. During training, it was also discovered that the omniscient latent variable phenomenon only appears on one single latent variable in

most training.

First, we define the omniscient latent variable as the probability that any dimension's information entropy in latent variables  $z$  of all trained models satisfies  $P[E_{q(z_i)}(-\log q(z_i)) < \epsilon] \geq 1 - \delta$  under a given parameter capacity and grouping factor. In this paper, we fix  $\epsilon$  as 0.001.

Fig. 5(b) shows that the omniscient latent variable appears at the top right in dSprites, while it is more concentrated at the top in the other two datasets. The reason for the difference is that the model was trained using MLP network on the dSprites dataset while using Conv network on the other two datasets. The overall parameter capacity of Conv is greater than MLP because the convolutional layer cannot alter parameter capacity, as designed in Appendix B.1. Therefore, it has a certain "basic" parameter capacity in Conv network. The omniscient latent variable appears in the upper right side of the figure, indicating this phenomenon occurs in the overfitting region of dependent features, which is in line with our definition of dependent features overfitting.

The MIG metric method uses the first-highest mutual information minus the second-highest mutual information to achieve a penalty for multiple variables containing same feature. However, if there are only two latent variables and one of them is an omniscient latent variable, then the second highest mutual information will always be 0, resulting in MIG distortion. Therefore, the  $\beta$ -STCVAE with only two latent variables should be avoided when calculating

MIG in the region where omniscient latent variables are present.

#### 4.4.2 Disentangling capability evaluation

The MIG disentangling measures of  $\beta$ -TCVAE and  $\beta$ -STCVAE under different parameter capacities and latent variable grouping coefficients are tested on the cars3d, dSprites, and shape3d, in Fig. 6. Model  $\beta$ -STCVAE takes the average value of MIG under all grouping coefficients except 1 (to avoid the MIG distortion caused by the omniscient latent variable).

Set the model referring to 4.4.1, and take the training model's average MIG. As shown in Fig. 6, the disentangling ability of  $\beta$ -STCVAE increases gradually with the increase of parameter capacity. In contrast, the disentangling ability of  $\beta$ -TCVAE increases very gently. We think the main reason is that under different parameter capacities,  $\beta$ -STCVAE can find the appropriate prior distribution of latent variables to accommodate the data features learned by encoder, while  $\beta$ -TCVAE cannot adjust the prior distribution of latent variables, which limits the disentangling learning ability.

The MIG disentangling metrics of  $\beta$ -STCVAE,  $\beta$ -TCVAE,  $\beta$ VAE, FactorVAE, and DIP-VAE-I are tested on 3 datasets under a fixed number of latent variables, as shown in Fig. 7. Setting model hyperparameter referring Appendix B.1 Table3. The dSprites dataset parameter capacity list is [3000, 4000, 5000]; cars3d parameter capacity list is [800, 900, 1000]; and shape3d parameter capacity list is [800, 1000, 1200]. The disentangling performance of  $\beta$ -STCVAE on these three datasets is better than that of the above VAE models clearly.

## 5 CONCLUSION

The notions of entangling and disentangling are complementary, and most previous research in the literature has concentrated on applying VAE disentangling properties. However, the feature disentangling degree of each person's subjective concept may vary. A dynamic disentangling prior distribution is created in this research by decomposing the independence constraints in multi-dimensional Gaussian distribution, allowing VAE to be used in more complex disentangling scenarios. The proposed approach creates a Macro and micro switchable unsupervised disentangling algorithm, which is more tally with human understanding. In the experiment, the best ELBO trajectory in parameter space is visualized, as are the characteristics of generated samples in corresponding regions, providing some suggestions for future work. It also demonstrates that the new method can provide more flexible disentangling performance. Furthermore, we design experiments to verify the TC estimate deviation theory proposed in this paper.

However, unified disentangling capability metrics for complex data features are still lacking. The data properties in the real world are unquestionably more complicated, but the evaluations of new methods are only being con-

ducted on toy datasets. In the future, we propose to describe the difference in disentangling degree produced by various subjective perspectives and provide a uniform disentangling metric for a practical application of unsupervised.

## REFERENCES

- [1] D. P. Kingma and M. Welling, "Auto-encoding variational bayes," arXiv preprint arXiv:1312.6114, 2013.
- [2] R. T. Chen, X. Li, R. B. Grosse, and D. K. Duvenaud, "Isolating sources of disentanglement in variational autoencoders," *Advances in neural information processing systems*, vol. 31, 2018.
- [3] G. Lee and H. Li, "Modeling code-switch languages using bilingual parallel corpus," in *Proceedings of the 58th Annual Meeting of the Association for Computational Linguistics*, 2020, pp. 860-870.
- [4] X. Chen, "Simulation of English speech emotion recognition based on transfer learning and CNN neural network," *Journal of Intelligent & Fuzzy Systems*, vol. 40, no. 2, pp. 2349-2360, 2021.
- [5] Y. Lü, H. Lin, P. Wu, and Y. Chen, "Feature compensation based on independent noise estimation for robust speech recognition," *EURASIP Journal on Audio, Speech, and Music Processing*, vol. 2021, no. 1, pp. 1-9, 2021.
- [6] Y. Shi, X. Yu, K. Sohn, M. Chandraker, and A. K. Jain, "Towards universal representation learning for deep face recognition," in *Proceedings of the IEEE/CVF Conference on Computer Vision and Pattern Recognition*, 2020, pp. 6817-6826.
- [7] T. Ni, X. Gu, C. Zhang, W. Wang, and Y. Fan, "Multi-task deep metric learning with boundary discriminative information for cross-age face verification," *Journal of Grid Computing*, vol. 18, no. 2, pp. 197-210, 2020.
- [8] X. Shi, C. Yang, X. Xia, and X. Chai, "Deep cross-species feature learning for animal face recognition via residual interspecies equivariant network," in *European Conference on Computer Vision*, 2020: Springer, pp. 667-682.
- [9] J. Chen, B. Lei, Q. Song, H. Ying, D. Z. Chen, and J. Wu, "A hierarchical graph network for 3d object detection on point clouds," in *Proceedings of the IEEE/CVF conference on computer vision and pattern recognition*, 2020, pp. 392-401.
- [10] A. S. Brown, S. Hornstein, and A. Memon, "Tracking conversational repetition: An evaluation of target monitoring ability," *Applied Cognitive Psychology: The Official Journal of the Society for Applied Research in Memory and Cognition*, vol. 20, no. 1, pp. 85-95, 2006.
- [11] Z. Xu, E. Hrustic, and D. Vivet, "Centernet heatmap propagation for real-time video object detection," in *European conference on computer vision*, 2020: Springer, pp. 220-234.
- [12] D. Zhang, H. Tian, and J. Han, "Few-cost salient object detection with adversarial-paced learning," *Advances in Neural Information Processing Systems*, vol. 33, pp. 12236-12247, 2020.
- [13] A. Torfi, R. A. Shirvani, Y. Keneshloo, N. Tavaf, and E. A. Fox, "Natural language processing advancements by deep learning: A survey," arXiv preprint arXiv:2003.01200, 2020.
- [14] S. Stoll, N. C. Camgoz, S. Hadfield, and R. Bowden, "Text2Sign: towards sign language production using neural machine translation and generative adversarial networks," *International Journal of Computer Vision*, vol. 128, no. 4, pp. 891-908, 2020.
- [15] P. He, X. Liu, J. Gao, and W. Chen, "Deberta: Decoding-enhanced bert with disentangled attention," arXiv preprint arXiv:2006.03654, 2020.
- [16] I. Higgins et al., "beta-vae: Learning basic visual concepts with a constrained variational framework," 2016.

- [17] A. Kumar, P. Sattigeri, and A. Balakrishnan, "Variational inference of disentangled latent concepts from unlabeled observations," arXiv preprint arXiv:1711.00848, 2017.
- [18] H. Kim and A. Mnih, "Disentangling by factorising," in International Conference on Machine Learning, 2018: PMLR, pp. 2649-2658.
- [19] M. Kim, Y. Wang, P. Sahu, and V. Pavlovic, "Relevance factor VAE: Learning and identifying disentangled factors," arXiv preprint arXiv:1902.01568, 2019.
- [20] F. Locatello et al., "Challenging common assumptions in the unsupervised learning of disentangled representations," in international conference on machine learning, 2019: PMLR, pp. 4114-4124.
- [21] S. Parekh, S. ESSID, A. Ozerov, N. Q. Duong, P. Pérez, and G. Richard, "Weakly supervised representation learning for audio-visual scene analysis," IEEE/ACM Transactions on Audio, Speech, and Language Processing, vol. 28, pp. 416-428, 2019.
- [22] F. Locatello, B. Poole, G. Rätsch, B. Schölkopf, O. Bachem, and M. Tschannen, "Weakly-supervised disentanglement without compromises," in International Conference on Machine Learning, 2020: PMLR, pp. 6348-6359.
- [23] J. Antoran and A. Miguel, "Disentangling and learning robust representations with natural clustering," in 2019 18th IEEE International Conference On Machine Learning And Applications (ICMLA), 2019: IEEE, pp. 694-699.
- [24] L. Bonheme and M. Grzes, "Be More Active! Understanding the Differences between Mean and Sampled Representations of Variational Autoencoders," arXiv preprint arXiv:2109.12679, 2021.
- [25] Y. Burda, R. Grosse, and R. Salakhutdinov, "Importance weighted autoencoders," arXiv preprint arXiv:1509.00519, 2015.
- [26] A. Vahdat and J. Kautz, "NVAE: A deep hierarchical variational autoencoder," Advances in Neural Information Processing Systems, vol. 33, pp. 19667-19679, 2020.
- [27] A. Shekhovtsov, D. Schlesinger, and B. Flach, "VAE Approximation Error: ELBO and Exponential Families," in International Conference on Learning Representations, 2021.
- [28] E. Dupont, "Learning disentangled joint continuous and discrete representations," Advances in Neural Information Processing Systems, vol. 31, 2018.
- [29] C. P. Burgess et al., "Understanding disentangling in  $\beta$ -VAE," arXiv preprint arXiv:1804.03599, 2018.
- [30] H. Shao et al., "Controlvae: Controllable variational autoencoder," in International Conference on Machine Learning, 2020: PMLR, pp. 8655-8664.
- [31] S. Zhao, J. Song, and S. Ermon, "Learning hierarchical features from deep generative models," in International Conference on Machine Learning, 2017: PMLR, pp. 4091-4099.
- [32] M. Willetts, S. Roberts, and C. Holmes, "Disentangling to cluster: Gaussian mixture variational Ladder autoencoders," arXiv preprint arXiv:1909.11501, 2019.
- [33] B. Esmaili et al., "Structured disentangled representations," in The 22nd International Conference on Artificial Intelligence and Statistics, 2019: PMLR, pp. 2525-2534.
- [34] D. Bouchacourt, R. Tomioka, and S. Nowozin, "Multi-level variational autoencoder: Learning disentangled representations from grouped observations," in Proceedings of the AAAI Conference on Artificial Intelligence, 2018, vol. 32, no. 1.
- [35] A. Szabo, Q. Hu, T. Portenier, M. Zwicker, and P. Favaro, "Understanding degeneracies and ambiguities in attribute transfer," in Proceedings of the European Conference on Computer Vision (ECCV), 2018, pp. 700-714.
- [36] Y. Ge, S. Abu-El-Haija, G. Xin, and L. Itti, "Zero-shot synthesis with group-supervised learning," arXiv preprint arXiv:2009.06586, 2020.
- [37] E. H. Sanchez, M. Serrurier, and M. Ortner, "Learning disentangled representations via mutual information estimation," in European Conference on Computer Vision, 2020: Springer, pp. 205-221.
- [38] P. Esser, J. Haux, and B. Ommer, "Unsupervised robust disentangling of latent characteristics for image synthesis," in Proceedings of the IEEE/CVF International Conference on Computer Vision, 2019, pp. 2699-2709.
- [39] D. Lorenz, L. Bereska, T. Milbich, and B. Ommer, "Unsupervised part-based disentangling of object shape and appearance," in Proceedings of the IEEE/CVF Conference on Computer Vision and Pattern Recognition, 2019, pp. 10955-10964.
- [40] K. Greff, A. Rasmus, M. Berglund, T. Hao, H. Valpola, and J. Schmidhuber, "Tagger: Deep unsupervised perceptual grouping," Advances in Neural Information Processing Systems, vol. 29, 2016.
- [41] Y. Li, K. K. Singh, U. Ojha, and Y. J. Lee, "Mixnmatch: Multifactor disentanglement and encoding for conditional image generation," in Proceedings of the IEEE/CVF conference on computer vision and pattern recognition, 2020, pp. 8039-8048.
- [42] C. Cremer, X. Li, and D. Duvenaud, "Inference suboptimality in variational autoencoders," in International Conference on Machine Learning, 2018: PMLR, pp. 1078-1086.
- [43] D. Hjelm, R. R. Salakhutdinov, K. Cho, N. Jojic, V. Calhoun, and J. Chung, "Iterative refinement of the approximate posterior for directed belief networks," Advances in neural information processing systems, vol. 29, 2016.
- [44] Y. Kim, S. Wiseman, A. Miller, D. Sontag, and A. Rush, "Semi-amortized variational autoencoders," in International Conference on Machine Learning, 2018: PMLR, pp. 2678-2687.
- [45] J. He, D. Spokoiny, G. Neubig, and T. Berg-Kirkpatrick, "Lagging inference networks and posterior collapse in variational autoencoders," arXiv preprint arXiv:1901.05534, 2019.
- [46] B. Dai, Z. Wang, and D. Wipf, "The usual suspects? Reassessing blame for VAE posterior collapse," in International Conference on Machine Learning, 2020: PMLR, pp. 2313-2322.
- [47] S. Nowozin, "Debiasing evidence approximations: On importance-weighted autoencoders and jackknife variational inference," in International conference on learning representations, 2018.
- [48] D. Rezende and S. Mohamed, "Variational inference with normalizing flows," in International conference on machine learning, 2015: PMLR, pp. 1530-1538.
- [49] R. Ranganath, D. Tran, and D. Blei, "Hierarchical variational models," in International conference on machine learning, 2016: PMLR, pp. 324-333.
- [50] B. Jiang, C. Ye, and J. S. Liu, "Nonparametric k-sample tests via dynamic slicing," Journal of the American Statistical Association, vol. 110, no. 510, pp. 642-653, 2015.
- [51] C. Granger and J. L. Lin, "Using the mutual information coefficient to identify lags in nonlinear models," Journal of time series analysis, vol. 15, no. 4, pp. 371-384, 1994.
- [52] P. Cheng et al., "Improving disentangled text representation learning with information-theoretic guidance," arXiv preprint arXiv:2006.00693, 2020.
- [53] R. D. Hjelm et al., "Learning deep representations by mutual information estimation and maximization," arXiv preprint arXiv:1808.06670, 2018.
- [54] D. J. Zea, D. Anfossi, M. Nielsen, and C. Marino-Buslje, "MIToS.jl: mutual information tools for protein sequence analysis in the Julia language," Bioinformatics, vol. 33, no. 4, pp. 564-565, 2017.

- [55] A. Lachmann, F. M. Giorgi, G. Lopez, and A. Califano, "ARACNe-AP: gene network reverse engineering through adaptive partitioning inference of mutual information," *Bioinformatics*, vol. 32, no. 14, pp. 2233-2235, 2016.
- [56] J.-F. Cardoso, "Dependence, correlation and gaussianity in independent component analysis," *The Journal of Machine Learning Research*, vol. 4, pp. 1177-1203, 2003.
- [57] P. Cheng, W. Hao, and L. Carin, "Estimating total correlation with mutual information bounds," *arXiv preprint arXiv:2011.04794*, 2020.
- [58] J. Lucas, G. Tucker, R. Grosse, and M. Norouzi, "Understanding posterior collapse in generative latent variable models," 2019.
- [59] S. E. Reed, Y. Zhang, Y. Zhang, and H. Lee, "Deep visual analogy-making," *Advances in neural information processing systems*, vol. 28, 2015.
- [60] L. Deng, "The mnist database of handwritten digit images for machine learning research [best of the web]," *IEEE signal processing magazine*, vol. 29, no. 6, pp. 141-142, 2012.

## APPENDIX A

### A.1 Total correlation Top-Down Tree-Like Path Decomposition

Suppose the dimension of  $z$  is  $n$ . Divide the dimension of  $z$  into  $Z_A$  and  $Z_{\bar{A}}$ , set  $Z_A := (z_{k1}, z_{k2}, z_{k3}, \dots, z_{km})$ ,  $Z_{\bar{A}} := (z_{v1}, z_{v2}, z_{v3}, \dots, z_{vt})$ , and have  $Z = Z_A \cup Z_{\bar{A}}$ ,  $Z_A \cap Z_{\bar{A}} = \emptyset$ , then:

$$\begin{aligned}
TC(Z) &= E_{p(Z)} \left[ \log \frac{p(z_1, z_2, z_3, \dots, z_n)}{p(z_1)p(z_2)\dots p(z_n)} \right] \\
&= E_{p(Z)} \left[ \log \left( \frac{p(Z_A)}{p(z_{k1})p(z_{k2})\dots p(z_{km})} \cdot \frac{p(Z_{\bar{A}})}{p(z_{v1})p(z_{v2})\dots p(z_{vt})} \right) \right. \\
&\quad \left. \cdot \frac{p(Z)}{p(Z_A)p(Z_{\bar{A}})} \right] \\
&= E_{p(Z)} \left[ \log \left( \frac{p(Z_A)}{p(z_{k1})p(z_{k2})\dots p(z_{km})} \right) \right. \\
&\quad \left. + E_{p(Z)} \left[ \log \left( \frac{p(Z_{\bar{A}})}{p(z_{v1})p(z_{v2})\dots p(z_{vt})} \right) \right] \right. \\
&\quad \left. + E_{p(Z)} \left[ \log \left( \frac{p(Z)}{p(Z_A)p(Z_{\bar{A}})} \right) \right] \right] \\
&= E_{p(Z_A)} \left[ p(Z_{\bar{A}}|Z_A) \cdot \log \left( \frac{p(Z_A)}{p(z_{k1})p(z_{k2})\dots p(z_{km})} \right) \right. \\
&\quad \left. + E_{p(Z_{\bar{A}})} \left[ p(Z_A|Z_{\bar{A}}) \cdot \log \left( \frac{p(Z_{\bar{A}})}{p(z_{v1})p(z_{v2})\dots p(z_{vt})} \right) \right] \right] + I(Z_A; Z_{\bar{A}}), \tag{18}
\end{aligned}$$

where  $E_{p(Z_A)} \left[ p(Z_{\bar{A}}|Z_A) \cdot \log \left( \frac{p(Z_A)}{p(z_{k1})p(z_{k2})\dots p(z_{km})} \right) \right]$  is not always the total correlation of  $Z_A$ .

Discuss according to the situation:

If  $Z_A$  and  $Z_{\bar{A}}$  are independent of each other:

$$\begin{aligned}
E_{p(Z_A)} \left[ p(Z_{\bar{A}}|Z_A) \cdot \log \left( \frac{p(Z_A)}{p(z_{k1})p(z_{k2})\dots p(z_{km})} \right) \right] \\
= TC(Z_A), \tag{19}
\end{aligned}$$

If  $Z_A$  and  $Z_{\bar{A}}$  are not independent of each other:

$$\begin{aligned}
E_{p(Z_A)} \left[ p(Z_{\bar{A}}|Z_A) \cdot \log \left( \frac{p(Z_A)}{p(z_{k1})p(z_{k2})\dots p(z_{km})} \right) \right] \\
= TC(Z_A) |_{q(Z)=q(Z_A) \cdot q(Z_{\bar{A}})}, \tag{20}
\end{aligned}$$

Where  $TC(Z_A) |_{q(Z)=q(Z_A) \cdot q(Z_{\bar{A}})}$  indicates that the importance sampling method is used to calculate the  $TC(Z_A)$  that satisfies the target distribution under the proposed distribution  $q(Z_A)$ . See Section 3.4 for detailed analysis.

Therefore:

$$\begin{aligned}
TC(Z) &= TC(Z_A) |_{q(Z)=q(Z_A) \cdot q(Z_{\bar{A}})} + TC(Z_{\bar{A}}) |_{q(Z)=q(Z_A) \cdot q(Z_{\bar{A}})} \\
&\quad + I(Z_A; Z_{\bar{A}}). \tag{21}
\end{aligned}$$

### A.2 Total Correlation Line-Like Path Decomposition

Suppose the dimension of  $z$  is  $n$ . Let  $Z_{i:j} := (z_i, z_{i+1}, \dots, z_{j-1}, z_j)$ , then we have:

$$\begin{aligned}
TC(Z_{1:n}) &= E_{p(Z)} \left[ \log \frac{p(z_1, z_2, z_3, \dots, z_n)}{p(z_1)p(z_2)\dots p(z_n)} \right] \\
&= E_{p(Z)} \left[ \log \left( \frac{p(z_1, z_2, z_3, \dots, z_n)}{p(z_1)p(z_2)\dots p(z_{n-1}) \cdot p(z_n)} \cdot \frac{p(z_1, z_2, z_3, \dots, z_{n-1})}{p(z_1)p(z_2)\dots p(z_{n-1})} \right) \right] \\
&= I(Z_{1:n-1}; Z_n) + E_{p(Z_{1:n-1})} \left[ p(Z_n|Z_{1:n-1}) \right. \\
&\quad \left. \cdot \log \left( \frac{p(z_1, z_2, z_3, \dots, z_{n-1})}{p(z_1)p(z_2)\dots p(z_{n-1})} \right) \right]
\end{aligned}$$

Discuss according to the situation:

If  $Z_n$  and  $Z_{1:n-1}$  are independent of each other:

$$\begin{aligned}
E_{p(Z_{1:n-1})} \left[ p(Z_n|Z_{1:n-1}) \cdot \log \left( \frac{p(z_1, z_2, z_3, \dots, z_{n-1})}{p(z_1)p(z_2)\dots p(z_{n-1})} \right) \right] \\
= TC(Z_{1:n-1}), \tag{22}
\end{aligned}$$

If  $Z_n$  and  $Z_{1:n-1}$  are not independent of each other:

$$\begin{aligned}
E_{p(Z_{1:n-1})} \left[ p(Z_n|Z_{1:n-1}) \cdot \log \left( \frac{p(z_1, z_2, z_3, \dots, z_{n-1})}{p(z_1)p(z_2)\dots p(z_{n-1})} \right) \right] = \\
TC(Z_{1:n-1}) |_{q(Z)=q(Z_n) \cdot q(Z_{1:n-1})}, \tag{23}
\end{aligned}$$

Same as A.1:  $TC(Z_{1:n-1}) |_{q(Z)=q(Z_n) \cdot q(Z_{1:n-1})}$  indicates that the importance sampling method is used to calculate the  $TC(Z_{1:n-1})$  that satisfies the target distribution under the proposed distribution  $q(Z_{1:n-1})$ .

Therefore:

$$\begin{aligned}
TC(Z_{1:n}) &= I(Z_{1:n-1}; Z_n) + TC(Z_{1:n-1}) |_{q(Z)=q(Z_n) \cdot q(Z_{1:n-1})} \\
&\quad \text{Continue to iterate:} \\
TC(Z_{1:n}) &= I(Z_{1:n-1}; Z_n) + I(Z_{1:n-2}; Z_{n-1}) |_{q(Z)=q(Z_n) \cdot q(Z_{1:n-1})} \\
&\quad + TC(Z_{1:n-2}) |_{q(Z)=q(Z_{n-1:n}) \cdot q(Z_{1:n-2})} \\
&= I(Z_{1:n-1}; Z_n) + \sum_{i=1}^{n-2} I(Z_{1:i}; Z_{i+1}) |_{q(Z)=q(Z_{\min(n,i+2);n}) \cdot q(Z_{1:i+1})} \tag{24}
\end{aligned}$$

Where  $\min(n, i+2)$  represents a small value among  $i+2$  and  $n$ .

It can be seen from objective (24) that at the end of the iterative solution, except for the first item  $I(Z_{1:n-1}; Z_n)$ , other items are based on importance sampling to obtain mutual information.

### A.3 Total Correlation Bottom-Up Tree-Like Path Decomposition

Suppose the total dimension of  $z$  in this proof is  $n$ .  $p(z_{-i:j})$  represents the joint probability of all dimensions except dimension  $z$ .

$$D_{KL}(q(z) || \prod_k q(z_k)) = \int_{-\infty}^{+\infty} q(z) \log \frac{q(z)}{\prod_k q(z_k)}. \tag{25}$$

Objective (25) is an improper integral with upper and lower bounds  $(-\infty, +\infty)$ . Since  $q(z)$  has no analytical formula, the solution  $\sigma$  of  $D_{KL}(q(z) || \prod_k q(z_k))$  can only be calculated using the sampling method.

When  $\sigma$  is a constant, it means that objective (25) converges, then the following derivation:

$$\begin{aligned}
D_{KL}(q(z) || \prod_k q(z_k)) &= \int_{-\infty}^{+\infty} q(z) \log \frac{q(z)}{\prod_k q(z_k)} \\
&= \lim_{\substack{u \rightarrow +\infty \\ v \rightarrow -\infty}} \int_v^u q(z) \log \frac{q(z)}{\prod_k q(z_k)} = \sigma, \tag{26}
\end{aligned}$$

Where  $\forall \varepsilon > 0$ ,  $\exists \alpha > 0$ . so that for  $\forall u > \alpha$ , and  $\forall v < -\alpha$ , there is  $|\int_v^u q(z) \log \frac{q(z)}{\prod_k q(z_k)} - \sigma| < \varepsilon$ . Therefore, it can be assumed that the probability density function of each dimension of the hidden variable  $z_i$  of the hidden space distribution  $z$  has a unified upper and lower limit  $(v, u)$  so that the gap between  $\int_v^u q(z) \log \frac{q(z)}{\prod_k q(z_k)}$  and  $D_{KL}(q(z) || \prod_k q(z_k))$  is smaller than an extremely small positive number  $\varepsilon$ .

Therefore, a definite integral with upper and lower

bounds can be used to replace the anomalous integral. For the sake of brevity, the integral symbol  $\int$  in the following derivation represents the definite integral to integrate all dimensions  $(z_1, z_2 \dots z_n)$  of  $z$  respectively.

$$\begin{aligned} D_{KL}(q(z) \parallel \prod_k q(z_k)) \\ &= \int q(z) \log \frac{q(z)}{\prod_k q(z_k)} \\ &= \int q(z_1, z_2) q(z_{-1,2} | z_1, z_2) \log \frac{q(z_1, z_2) q(z_{-1,2} | z_1, z_2)}{\prod_k q(z_k)} \\ &= \int q(z_1, z_2) \log \frac{q(z)}{q(z_1) q(z_2)} q(z_{-1,2} | z_1, z_2) + \\ &\quad \boxed{\int q(z) \log \frac{q(z)}{\prod_{\substack{k \neq 1 \\ k \neq 2}} q(z_k) \cdot q(z_1, z_2)}} \end{aligned} \quad (27)$$

Where the box in objective (27) can be decomposed as:

$$\begin{aligned} &= \int q(z_3, z_4) q(z_{-3,4} | z_3, z_4) \log \frac{q(z_3, z_4) q(z_{-3,4} | z_3, z_4)}{\prod_{\substack{k \neq 1 \\ k \neq 2}} q(z_k) \cdot q(z_1, z_2)} \\ &= \int q(z_3, z_4) \log \frac{q(z_3, z_4)}{q(z_3) q(z_4)} q(z_{-3,4} | z_3, z_4) + \\ &\quad \boxed{\int q(z) \log \frac{q(z_1, z_2 \dots z_n)}{\prod_{\substack{k \neq 1 \\ k \neq 2 \\ k \neq 3 \\ k \neq 4}} q(z_k) \cdot q(z_1, z_2) \cdot q(z_3, z_4)}} \end{aligned} \quad (28)$$

We can continue to decompose the box in objective (28). Finally, we get an objective that needs to be discussed in different situations.

If  $n$  is even, then:

$$\begin{aligned} &= \int q(z_1, z_2) \log \frac{q(z_1, z_2)}{q(z_1) q(z_2)} q(z_{-1,2} | z_1, z_2) \\ &+ \int q(z_3, z_4) \log \frac{q(z_3, z_4)}{q(z_3) q(z_4)} q(z_{-3,4} | z_3, z_4) + \dots \\ &+ \boxed{\int q(z) \log \frac{q(z)}{q(z_1, z_2) \cdot q(z_3, z_4) \dots q(z_{n-1}, z_n)}} \end{aligned} \quad (29)$$

If  $n$  is odd, then:

$$\begin{aligned} &= \int q(z_1, z_2) \log \frac{q(z_1, z_2)}{q(z_1) q(z_2)} q(z_{-1,2} | z_1, z_2) \\ &+ \int q(z_3, z_4) \log \frac{q(z_3, z_4)}{q(z_3) q(z_4)} q(z_{-3,4} | z_3, z_4) + \dots \\ &+ \boxed{\int q(z) \log \frac{q(z)}{q(z_1, z_2) \cdot q(z_3, z_4) \dots q(z_{n-2}, z_{n-1}) \cdot q(z_n)}} \end{aligned} \quad (30)$$

When the box in objective (29) is equal to 0, it means that except for the last item, all the  $q(z_i, z_j)$  joint distributions that appear in the previous items are independent.

At this situation, there are:

$$\begin{aligned} \int q(z_i, z_j) \log \frac{q(z_i, z_j)}{q(z_i) q(z_j)} q(z_{-i,j} | z_i, z_j) &= E_{q(z)} \left[ \log \frac{q(z_i, z_j)}{q(z_i) q(z_j)} \right] \\ &= \int q(z_i, z_j) \log \frac{q(z_i, z_j)}{q(z_i) q(z_j)} q(z_{-i,j}) \\ &= \int q(z_i, z_j) \log \frac{q(z_i, z_j)}{q(z_i) q(z_j)} \\ &= I(z_i; z_j) = E_{q(z_i, z_j)} \left[ \log \frac{q(z_i, z_j)}{q(z_i) q(z_j)} \right] \end{aligned}$$

Where  $i \neq j$ ,  $i$  and  $j < n$ . When the box in objective (29) is not equal to 0, it means that except for the last item, all the joint distributions  $q(z_i, z_j)$  appearing in the previous

items are not independent. There are:

$$\begin{aligned} \int q(z_i, z_j) \log \frac{q(z_i, z_j)}{q(z_i) q(z_j)} q(z_{-i,j} | z_i, z_j) \\ &= E_{q(z)} \left[ \log \frac{q(z_i, z_j)}{q(z_i) q(z_j)} \right] \\ &= E_{q(z_i, z_j)} \left[ q(z_{-i,j} | z_i, z_j) \cdot \log \frac{q(z_i, z_j)}{q(z_i) q(z_j)} \right] \end{aligned}$$

Intuitively,  $E_{q(z_i, z_j)} \left[ q(z_{-i,j} | z_i, z_j) \cdot \log \frac{q(z_i, z_j)}{q(z_i) q(z_j)} \right]$  can be regarded as the importance sampling of  $E_{q(z)} \left[ \log \frac{q(z_i, z_j)}{q(z_i) q(z_j)} \right]$ , taking  $q(z_{-i,j} | z_i, z_j)$  as the importance weight. The importance weight is 1, when  $q(z_{-i,j})$  and  $q(z_i, z_j)$  are independent of each other. As a result, when  $q(z_i, z_j)$  and  $q(z_{-i,j})$  are not independent, it can be viewed as a way of describing  $I(z_i; z_j)$  by importance sampling. The situation in objective (30) is similar.

Assuming that the latent variable  $z$  has  $n$  dimensions,  $z_i$  represents the  $i$  th dimension in the latent variable.  $cp(i, j)$  Represents a mechanism for selecting a pair of latent variables  $z_i, z_j$  without replacement, and the  $cp(i, j)$  in the summation symbol is consistent with the result of the  $cp(i, j)$  in the cumulative multiplication symbol;  $z_r$  represents the final remaining latent variable  $r$  after selecting several times without replacement under the odd case  $cp(i, j)$ :

$$\begin{aligned} TC(z) &= D_{KL}(q(z) \parallel \prod_k q(z_k)) = \\ &\left\{ \begin{array}{l} \sum_{cp(i,j)} E_{q(z)} \left[ \log \frac{q(z_i, z_j)}{q(z_i) q(z_j)} \right] + D_{KL}(q(z) \parallel \prod_{cp(i,j)} q(z_i, z_j)) \quad , n \text{ is even} \\ \sum_{cp(i,j)} E_{q(z)} \left[ \log \frac{q(z_i, z_j)}{q(z_i) q(z_j)} \right] + D_{KL}(q(z) \parallel \prod_{cp(i,j)} q(z_i, z_j) \cdot q(z_r)) \quad , n \text{ is odd} \end{array} \right. \end{aligned}$$

Where  $E_{q(z)} \left[ \log \frac{q(z_i, z_j)}{q(z_i) q(z_j)} \right]$  can be regarded as calculating  $I(z_i; z_j)$  using importance sampling, thus:

$$\begin{aligned} TC(z) &= \\ &\left\{ \begin{array}{l} \sum_{cp(i,j)} I(z_i; z_j) |_{q(z)=q(z_i, z_j) \cdot q(z_{-i,j})} + D_{KL}(q(z) \parallel \prod_{cp(i,j)} q(z_i, z_j)) \quad , n \text{ is even} \\ \sum_{cp(i,j)} I(z_i; z_j) |_{q(z)=q(z_i, z_j) \cdot q(z_{-i,j})} + D_{KL}(q(z) \parallel \prod_{cp(i,j)} q(z_i, z_j) \cdot q(z_r)) \quad , n \text{ is odd} \end{array} \right. \end{aligned}$$

Where the  $q(z_i, z_j)$  and  $q(z_{-i,j})$  in the target distribution are independent, but they are not necessarily independent in the proposed distribution.  $I(z_i; z_j) |_{q(z)=q(z_i, z_j) \cdot q(z_{-i,j})}$  indicates that the importance sampling method is used to calculate the  $I(z_i; z_j)$  that satisfies the target distribution under the proposed distribution  $q(z_i, z_j)$ .

Then set  $TC_{joint\_1}(z)$  as:

$$\begin{aligned} TC_{joint\_1}(z) &= \left\{ \begin{array}{l} D_{KL}(q(z) \parallel \prod_{cp(i,j)} q(z_i, z_j)) \quad , n \text{ is even} \\ D_{KL}(q(z) \parallel \prod_{cp(i,j)} q(z_i, z_j) \cdot q(z_r)) \quad , n \text{ is odd} \end{array} \right. \end{aligned}$$

We replace  $\sum_{cp(i,j)} I(z_i; z_j) |_{q(z)=q(z_i, z_j) \cdot q(z_{-i,j})}$  with  $MU_{joint\_1}(z)$ , Then  $TC_{joint\_1}(z) = TC(z) - MU_{joint\_1}(z)$ .

From objective (2), Knowing  $MU_{joint\_1}(z)$  is always

positive, defined as the accumulation of mutual information. Thus, the total correlation of the joint distribution must be less than or equal to the total correlation of the marginal distribution, which can be represented as  $TC_{joint_1}(z) \leq TC(z)$ .

The decomposition has an iterative relationship and can continue by treating  $TC_{joint_1}(z)$  as a new  $TC(z)$ . The joint distribution  $q(z_i, z_j)$  selected by  $cp(i, j)$  in the  $TC_{joint_1}(z)$  is regarded as the new latent variable set  $\{q(z_{1,1}), q(z_{1,2}) \dots q(z_{1,n/2})\}$  ( $(n+1)/2$  variables in total when  $n$  is odd, and  $n/2$  in total when  $n$  is even), thus we have:

$$TC_{joint_2}(z) = TC_{joint_1}(z) - MU_{joint_2}(z),$$

$$TC_{joint_3}(z) = TC_{joint_2}(z) - MU_{joint_3}(z),$$

....

Finally, there is the following objective:

$$TC(z) = MU_{joint_1}(z) + MU_{joint_2}(z) + \dots + I(z_{f-1}; z_{f,2}),$$

Where  $f = \text{int}(\log_2 n) - 2$ . If  $f < 1$ , then  $z_{f,i} = z_i$ , and  $n$  is the total dimension of  $z$ , and  $\text{int}(c)$  is the rounded-up integer of  $c$ .

Only two joint distribution variables will be left in the final round of decomposition regardless of the parity of  $n$ . In objective (5), the remaining joint distribution of the last term is represented by  $z_{f-1}$  and  $z_{f,2}$ .  $z_{f-1}$  and  $z_{f,2}$  are the two joint distributions composed of the marginal distributions selected by the  $cp(i, j)$  of the  $f$ th round. Notice that, only the mutual information  $I(z_{f-1}; z_{f,2})$  obtained in the last round of decomposition is not based on importance sampling. All  $MU_{joint_x}(z)$  are based on importance sampling.

## APPENDIX B

### B.1 Experimental Model Design Details

The main experiment's neural network model is divided into two types: MLP model and Conv model. dSprites, mnist and celebA are trained with MLP neural network, cars3d, shape3d are trained with Conv neural networks. The parameter capacities in the encoder and decoder are variable in order to make it easier to observe model's various parameter capacities. In Table1 and Table2 "Layer" represents the number of hidden layers in model; "neuron\_num" represents the number of neurons in a single layer, also the value in "parameter capacity list" in the main body and Table 4. The neuron\_num and layer variables determine the parameter capacity of the model. For other hyperparameters of the model, we refer to the experimental settings in F. Locatello's work[20].

TABLE 1  
MLP Model

Encoder	Decoder
Input: width * hight * channel	Input: $Latent\_dim$
FC $neuron\_num, ReLU$	FC $neuron\_num, Tanh$
FC $neuron\_num, ReLU * layer$	FC $neuron\_num, Tanh * layer$
FC $Latent\_dim * 2$	FC width * hight * channel
	Reshape width * hight * channel

$neuron\_num, Latent\_dim, layer$  are Parameters to be preset

\*  $layer$  Represent the number of repetitions of this layer

TABLE 2  
Conv Model

Encoder	Decoder
Input: $64*64* channel$	Input: number of $Latent\_dim$
$4*4$ conv,16 LeakyReLU, stride 2	FC $neuron\_num, Tanh * layer$
$4*4$ conv,32 LeakyReLU, stride 2	FC $8*8*64, Tanh$
$4*4$ conv,64 LeakyReLU, stride 2	$4*4$ upconv,32 LeakyReLU, stride 2
FC $neuron\_num, ReLU * layer$	$4*4$ upconv,16 LeakyReLU, stride 2
FC number of $Latent\_dim * 2$	$4*4$ upconv, channel LeakyReLU, stride 2

$neuron\_num, Latent\_dim, layer$  are Parameters to be preset

\*  $layer$  Represent the number of repetitions of this layer

TABLE 3  
Hyperparameter settings of different VAE models

Model	Parameter	Value
$\beta - STCVAE,$	$\beta$	[1,2,4,6,8,10]
$\beta - TCVAE,$		
$\beta VAE$		
FactorVAE	$\gamma$	[10,20,40,60,80,100]
DIP-VAE-I	$\lambda_{od}$	[1,2,5,10,20,50]
	$\lambda_d$	10 $\lambda_{od}$

TABLE 4  
Model and parameter capacity selection for different training sets

dataset	model	Hidden layer	Parameter capacity list
mnist	MLP	1layer	[20,40,60,80,100,200,300,400,500,1000,1500,2000,2500,3000,3500,4000,4500,5000]
celebA	MLP	1layer	[500,1000,1500,2000,2500,3000,3500,4000,4500,5000]
dSprite	MLP	1layer	[100,500,1000,1500,2000,2500,3000,3500,4000,4500,5000]
Cars3D	Conv	2layer	[100,200,300,400,500,600,700,800,900,1000]
shape3D	Conv	2layer	[200,300,400,500,600,700,800,900,1000,1100,1200]